Crossover Region of Dynamic Glass Transition in Poly(*n*-hexyl methacrylate) by Heat Capacity Spectroscopy

M. Beiner, S. Kahle, E. Hempel, K. Schröter, and E. Donth*

Fachbereich Physik, Universität Halle, D-06099 Halle (Saale), Germany

Received May 12, 1998; Revised Manuscript Received September 1, 1998

ABSTRACT: The crossover region of the dynamic glass transition in poly(*n*-hexyl methacrylate), PnHMA, was investigated by heat capacity, dielectric, and shear spectroscopy. Two distinct parts of the dynamic glass transition were observed in the calorimetric data, surprisingly separated by a saddle in the $c_p''(\log f,T)$ contour map at $\log(f/\mathrm{Hz}) = 0.33$ and $T = 2$ °C. The high temperature process *a*, above the saddle, is characterized by nearly temperature independent Δc_p values and a very small but constant cooperativity. Its calorimetric relaxation strength dies off above the saddle. The conventional cooperative α relaxation sets on about one frequency decade below. Its calorimetric relaxation strength Δc_p and cooperativity N_α strongly increases with decreasing temperature. The calorimetric onset of the α relaxation in the crossover region is confirmed by an additive analysis of dielectric data using two Havriliak−Negami functions. The results are discussed with respect to cooperativity as a function of temperature.

I. Introduction

The microscopic picture of slow relaxations in complex systems[1−3] is still poorly understood. New experimental approaches seem still necessary. Linear response is of general interest because it can directly be reduced to thermal fluctuation in equilibrium. Dynamic entropy compliance, c_p^*/T, from heat capacity spectroscopy (HCS) is of particular interest since entropy fluctuation seems directly be connected with cooperatively rearranging molecules.[4]

The crossover region is important for understanding of dynamic glass transition or main relaxation. Seen from lower temperature, this can be defined as the region where the low temperature part of the main relaxation, α, and the secondary Johari Goldstein relaxation, *β*,[5] approach each other. Several properties of the relaxation processes change there. (i) The temperature dependence of viscosity[6] and of dielectric main relaxation times[7] in glasses with weak *β* relaxation indicate that the WLF parameters, characterizing the underlying cooperativity, change in the crossover region from one set to another. (ii) Rotational and translational diffusion coefficients decouple[8] below the crossover region. (iii) Analyzing dielectric isotherms by additive α and *β* compliances, an onset of the α relaxation from zero intensity was obtained in the crossover region for a number of glasses with different chemical structures.[9−14]

In spite of increasing interest in the crossover,[7−15] it is still an open question what the basic reason for all the changes is. We can ask how the cooperativity behaves in the crossover. This can be deduced from HCS. This spectroscopy has the advantage of being not sensitive to secondary *β* relaxations ($\Delta c_p(\beta) \approx 0$,[16] apart from some biopolymers[17]). This avoids two problems of dielectric spectroscopy in the crossover region: (i) overlap of α and *β* loss peaks (fit problem) and (ii) decoupling of the two relaxation processes by differing models.[18] First calorimetric experiments by conventional DSC[19] and HCS[10,20,21] indicated a linear decrease of the step height, $\Delta c_p(T)$, when the crossover region is approached from below. This allows a simple extrapolation to a calorimetric α onset temperature T_{on}, where $\Delta c_p \rightarrow 0$. The dynamic heat capacity data can be represented as a surface over the log frequency-temperature plane, $c_p^*(\log f, T)$. Its behavior above the α onset and the details near the onset, i.e., in the crossover region, remained unknown so far.

Two main problems of such experiments are (i) finding a substance having the crossover region in the frequency-temperature HCS window and (ii) the realization of measurements in a large frequency-temperature range which are precise enough for detecting small and wide $c_p''(\log f,T)$ peaks.

The homologous series of the poly(n-alkyl methacrylate)s has been known for a long time[22,23] to have an *αβ* splitting which shifts systematically to lower frequencies/temperatures if the length of the alkyl side chain increases. Reanalyzing previous results,[9,19,21−24] we have chosen poly(*n*-hexyl methacrylate), PnHMA. Its crossover region is in the middle of the HCS frequency window. We used the 3*ω* method of Birge and Nagel[25,26] with a frequency window from 100mHz to some kHz. The comparison of typical HCS signal parameters for PnHMA with other glasses (Table 1) shows that HCS in the crossover region really requires a high signal quality. The amplitudes to be detected are ten times smaller and the peaks are three times wider as typical for the dynamic glass transition of good glass formers with T_g far below the crossover region. Wide glass transformation intervals cannot easily be detected because the measurements must be extended over a huge temperature range. This is an additional problem because a continuous heater-sample contact must be realized from far below to far above the glass temperature T_g. The experimental methods to overcome these problems are shortly described in the experimental part and are extensively discussed in ref 27.

In this paper we report on, to our knowledge, the first measurements of the dynamic heat capacity $c_p^*(\log f, T)$ in the crossover region of a glass former, the polymer poly(*n*-hexyl methacrylate) PnHMA. The calorimetric results are compared with dielectric and dynamic mechanical data in a comparable frequency−temperature range and are discussed with respect to cooperativity behavior in the crossover region.

10.1021/ma980754m CCC: $15.00
Published on Web 11/17/1998

Table 1. Calorimetric Characteristics of the Dynamic Glass Transition for the $f = 20$ Hz Isochron of Several Glass Formers Having Different Distances from the Onset[a]

substance[b]	T_{20}/K	log (f_{on}/20 Hz)[c]	$\Delta\check{c}_p/\check{c}_p$	tan δ_{max}	δT/K	N_α	refs
Glycerol	209	7	0.56	0.17	6	40	25, 27
PVAC	330	7	0.27	0.10	6	40	27, 46
SBR 1500	234	3.5	0.12	0.021	6	14	27
Co 8%	326	1.5	0.16	0.032	15	3	10
PnHMA	284	−1	0.07	0.018	20	0.7	this work
uncertainty	±2	±1	±10%	±0.005	±15%	±40%	

[a] T_{20} = temperature of the $\check{c}_p''(T)$ maximum for $f = 20$Hz, f_{on} = frequency of α onset, $\Delta\check{c}_p = \check{c}_p^{l}$(liquid zone for $T \gg T_{20}$) − $\check{c}_p^{glass}$ (glass zone for $T \ll T_{20}$), $c_p = (\check{c}_p^{l} + \check{c}_p^{glass})/2$ at T_{20}, tan δ_{max} c_p''/c_p' at T_{20}, δT = Gauss dispersion from a Gauss fit of the isochronous $\check{c}_p''$ peak, $\check{c}_p''(T) \sim \exp(-(T - T_{20})^2/2(\delta T)^2)$, and , N_α = cooperativity calculated from eq.1 [b] PVAC = polyvinylacetate, SBR 1500 = the random copolymer of styrene−butadiene rubber with 23% weight styrene, Co 8% the random copolymer of *n*-butylmethacrylate with 8% mole styrene, PnHMA = poly (*n*-hexyl methacrylate). [c] log = $\log_{10}$ always.

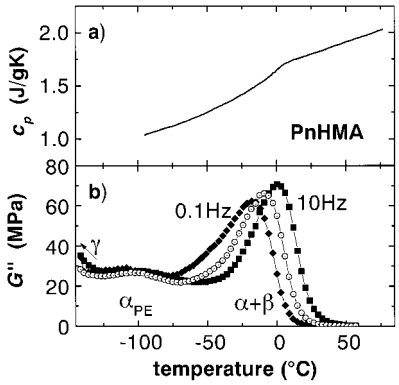

Figure 1. (a) Specific heat capacity of poly(*n*-hexyl methacrylate) in the glass transition region. The DSC curve was recorded at a heating rate of 20 K/min after cooling with the same rate. (b) Shear loss modulus G'' vs temperature for PnHMA at three frequencies (◆, 0.1 Hz; ⊙, 1 Hz; ■, 10 Hz). The different relaxation processes are indicated by γ, α_{PE}, and $\alpha + \beta$.

II. Experimental Section

A. Sample. The PnHMA sample was kindly provided by Dr. G. Meier (MPI für Polymerforschung Mainz). It is the same sample as investigated by dynamic light scattering and other methods in refs 28 and 29. The polymer was prepared by thermal polymerization of the filtered monomer by Röhm AG (Darmstadt, Germany). The average molecular weight is $\bar{M}_w = 1.6 \times 10^5$ g/mol and the polydispersity $\bar{M}_w/\bar{M}_n = 2.1$ (GPC with THF as eluent). The tacticity of the sample, soluted in nondeuterated THF, was obtained by ^{13}C NMR with a Varian 400 spectrometer. The sample has 78 ± 4% syndiotactic diades. The glass temperature from conventional DSC measurements by a Perkin-Elmer DSC7 at a heating rate of $\dot{T} = +20$ K/min is $T_g = -19 \pm 2$ °C. The corresponding thermograms have a very broad transformation interval, $\Delta T \approx 40$ K (Figure 1a). Further details of DSC on PnHMA are discussed in ref 30. The shear loss modulus G'' visualizes the complexity of the relaxation spectrum of PnHMA (Figure 1b). Besides the α (or better $\alpha + \beta$, see below) peak near T_g a secondary peak at about $T = -100$ °C is observed. This relaxation process (α_{PE}) was discussed as an additional polyethylene-like glass transition in poly(*n*-alkylmethacrylate)s with long alkyl groups in the side chain.[31] The maximum of the γ relaxation (T_γ (1 Hz)≈ −180 °C[31]) is outside our temperature window. To remove moisture, the samples were dried under vacuum for at least 12 h at $T = 100$ °C prior to the measurements. After this procedure, the dielectric, mechanical, and calorimetric properties were immediately measured in a dry nitrogen atmosphere.

B. Methods. HCS was performed by a home-made setup[32] using the 3ω method according to Birge and Nagel.[25] The quantity measured by this method is the product of density ρ, thermal conductivity κ, and dynamic heat capacity: $\rho\kappa c_p^*(\log f, T) = \rho\kappa(c_p' - ic_p'')$. Density and thermal conductivity are usually real quantities that practically do not depend on frequency.[33] The relative change of the thermal conductivity $\kappa(T)$ in the temperature interval from −75 to +75 °C is about 20%.

The details of the 3ω method, our setup, and the improvements are described in ref 27. Two main improvements are as follows: (i) The first is introduction of a new substrate material with very small $\rho\kappa c_p$ values, poly(ether ether ketone) PEEK ($T_g \approx 143$ °C). This results in a large (about 10×) increase of the useful signal amplitude compared to window glass substrates as used by other authors. (ii) The second is application of a sampling oscillograph in combination with a selective Fourier transformation (a fit of the raw voltage data with a superposition of only two sine components, $U_{3\omega}$ and U_ω). This procedure significantly increases the phase angle stability.

HCS on our polymeric glasses requires an extremely good heater-to-sample contact in a huge temperature range over long times. Even a "microscopic" separation of the sample from the heater surface leads to troublesome steps in the $\rho\kappa c_p^*(T)$ curves because the penetration depth of temperature waves is small, especially at high frequencies (about 15 μm at 2 kHz). The necessary adhesion was achieved by annealing the sample-heater-substrate sandwich at 85 °C for 3 days. Our PnHMA slowly flows under this conditions which leads to a "microplugging" between sample and the rough surface of the PEEK substrate around the nickel heater. This procedure and a slight pressure on the sample during the measurements guarantied a continuous sample-heater contact also when internal strains appeared below T_g.

The heater size was about 3 × 7 mm^2 and the sample thickness about 3 mm for HCS in the frequency range from 0.2 to 6Hz. Heaters of about 1.4 × 4.7 mm^2 and a sample thickness of about 1 mm were used in the frequency range from 2 to 2000 Hz. The heater resistance at room temperature was about 25Ω for both heaters, the substrate thickness was about 5mm and the relative temperature coefficient of resistance α_R at room temperature about 1650 ppm/K. Two independent HCS measurements were carried out on both heaters. Each data point was recorded two times per measurement; i.e., each $\rho\kappa c_p^*(\log f, T)$ value was measured at least four times and in the frequency overlap region up to eight times. The annealing time prior to the isothermal frequency sweeps was always 900 s. On each substrate, one run was started at the lowest temperature and the other run at the highest temperature. No systematic deviation in the experimental data was observed for these two equilibrating conditions; i.e., no influence of the temperature program was observed.

A commercial Novocontrol dielectric spectrometer using a Schlumberger frequency analyzer FRA1260 with active preamplifier on the cell was used for dielectric measurements. The diameter of the capacitor was 20 mm, the plate distance about 100 μm.

Deformation-controlled dynamic shear measurements were performed with a commercial rheometer RDAII from Rheometric Scientific. The strain amplitude was varied in the range from 0.2 to 0.5%. The linearity of the response was checked by isothermal strain sweeps. Stripe geometry was used. The dimensions of the sample were 1.5 × 10 × 25 mm^3. The G^* absolute values are comparatively uncertain because of nonideal sample geometry.

III. Results

Figure 2 shows raw HCS data for PnHMA from two independent isochronous scans (constant frequency of

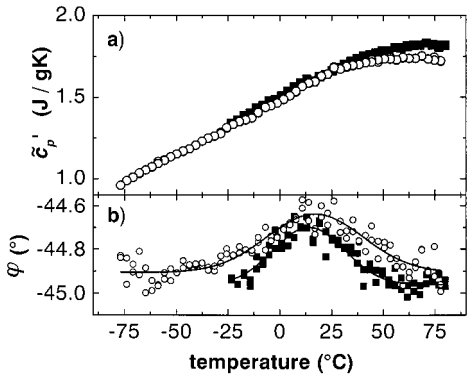

Figure 2. Heat capacity spectroscopy (HCS) data of PnHMA in the dynamic glass transition region. The two curves in both figures represent independent runs at constant frequency $f =$ 60 Hz. (a) Raw data for the real part $\tilde{c}_p'$ as calculated from the 3ω signal amplitude and calibrated to the specific heat from DSC (see text). (b) Raw data for the 3ω signal phase angle φ containing the information on the imaginary part c_p''. The solid lines are Gaussian adjustments with dispersions of δT = 17 K and δT = 23 K, respectively.

60 Hz) in order to demonstrate the reproducibility. The upper part (a) shows the real part of the HCS output $\rho\kappa c_p'$ as calculated from the third harmonic voltage $U_{3\omega}$ for the sample-heater-substrate sandwich and the empty substrate as a function of temperature. To get specific heat capacities, the $\rho\kappa c_p'$ data were reduced to absolute c_p values from conventional DSC (vitrification) measurements (Figure 1a). The data of both $\rho\kappa c_p'(T)$ measurements were multiplied by a frequency and temperature independent factor representing the ratio of the half step height values from DSC and HCS: $(\tilde{c}_p'/(\mathrm{Jg^{-1}K^{-1}}) = \rho\kappa c_p'/(\mathrm{J^2cm^{-4}K^{-2}s^{-1}}) \times 1.57/3.537 \times 10^{-3})$. The raw data of the third harmonic phase angle φ as a function of temperature display the small and wide peaks expected (Figure 2b). This quantity contains the information about the imaginary part $\rho\kappa c_p''$. The peak shapes from the two measurements shown are similar. Each $\varphi(T)$ peak can be fitted by one single Gaussian function. Their temperature dispersions, δT, are only slightly different (see figure caption). Both primary signals, $U_{3\omega}$ and φ, are sufficiently reproducible to give a significant indication for a relaxation process at T(60 Hz) $\approx$ 17 °C: the real part has a steplike transition, almost degenerated to a bend, and the imaginary part has a peak.

Figure 3a displays the imaginary component $\rho\kappa c_p''$ for PnHMA as function of temperature at nine different frequencies. The data are corrected by a linear base line to get $c_p'' \approx 0$ for low and high temperatures outside the peaks. Two independent isochronous measurements were averaged and FFT filter smoothed. For reasons of clarity only each fourth point is shown. Significant peaks in the $\rho\kappa c_p''(T)$ curves are observed at all frequencies. Peak heights and shapes at higher frequencies ($f >$ 6 Hz) are similar, while at lower frequencies ($f <$ 2 Hz) the peak height increases significantly. The temperature dispersion δT is large for all frequencies. It ranges from 15 to 20 K for PnHMA, while δT values of about 6 K are typical for conventional glasses like glycerol or polyvinylacetate (see Table 1). A complete set of fit parameters for the isochronous PnHMA data is listed in Table 2.

The real-part isochrones of the HCS output, $\rho\kappa c_p'$, at seven different frequencies in the range from 0.2 to 200 Hz are shown in Figure 3b. No clear steplike transformation, as otherwise typical for the dynamic glass transition, is observed for PnHMA at higher frequencies ($f >$ 2 Hz). Instead a degenerated, bendlike transformation is observed at temperatures between 15 and 35 °C. Indications for a steplike glass transition, however, were observed at the lower frequencies ($f <$ 0.6 Hz). This finding corresponds to the increasing $\rho\kappa c_{p_{\max}}''$ values at low frequencies in Figure 3a. All data points above the DSC glass transition temperature $T_g = -19$ °C are in thermodynamic equilibrium; e.g., these points are not affected by vitrification. The slight vertical shift of the low frequency isochrones (Figure 3b) results probably from a systematic error of the $\rho\kappa c_p'$ measurements on different substrates and an increasing influence of finite heater width and sample thickness at low frequencies. The low-frequency trend in the $\rho\kappa c_p''$ peak intensity,

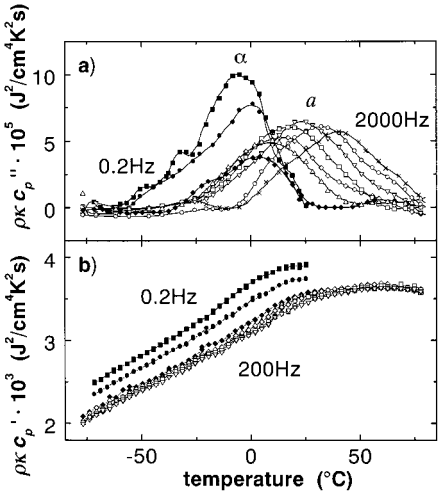

Figure 3. HCS data versus temperature for PnHMA at nine frequencies (■, 0.2; ●, 0.6; ◆, 2; △, 6; ◇, 20; □, 60; ▽, 202; ○, 600; ×, 2000 Hz). (a) The imaginary component $\rho\kappa c_p''$ as used for the construction of the contour maps and spectra, Figures 4b and 6. The isochrones were obtained in the following way: The raw phase angle data were corrected by a base line, averaged, FFT (fast Fourier transformation) filter smoothed to improve the signal-to-noise ratio, and finally thinned out by a factor of 4 for better representation. (b) The real part $\rho\kappa c_p'$ as measured by HCS. The isochrones above 2 Hz were measured on the small, and the 0.2 and 0.6 Hz curves on the large nickel heater.

Table 2. Calorimetric Parameters for PnHMA As Obtained from HCS (upper part) and DSC (lower part)

f/Hz	T_α/°C	δT/K	$\rho\kappa c_{p_{\max}}'' \times 10^5$/ $\mathrm{J^2\,K^{-2}\,cm^{-4}\,s^{-1}}$	$\Delta\tilde{c}_p$/ $\mathrm{J\,g^{-1}\,K^{-1}}$	N_α
2000	39.6	20.9	5.8	0.10	0.4
600	33.7	21.2	7.2	0.14	0.6
600	30.8	21.0	6.1	0.12	0.5
200	26.3	23.1	6.8	0.16	0.6
200	21.4	18.2	6.2	0.13	0.7
60	18.6	21.5	6.4	0.16	0.6
60	15.2	17.2	6.6	0.14	0.8
20	14.9	16.1	5.2	0.11	0.7
20	10.8	20.9	5.8	0.17	0.7
6	8.0	18.1	5.8	0.15	0.8
6	3.9	11.2	3.7	0.07	0.9
2	3.5	13.4	3.3	0.08	1.0
2	4.9	10.9	4.2	0.07	1.0
2	−2.5	15.3	4.6	0.13	0.9
0.6	−7.5	18.6	8.0	0.31	1.4
0.2	−7.1	14.2	8.8	0.26	1.8
0.2	−8.2	14.8	9.1	0.29	1.8
$\dot{T}$ = 20 K/min	−18	7.3		0.24	5.8
$\dot{T}$ = 20 K/min	−20	7.3		0.29	7.8

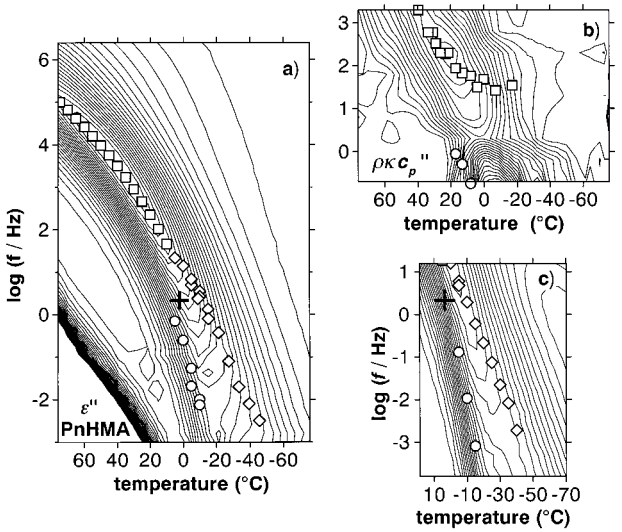

Figure 4. Comparison of dielectric (a), calorimetric (b), and mechanical (c) contour maps of the imaginary parts for PnHMA. The calorimetric map shows a saddle between the *a* death and the α onset. The dielectric and mechanical maps have no saddle there (cross). The dielectric onset details are hidden under a large β activity obviously absent in the calorimetric map. The temperature uncertainty between the three devices is ±2 K. The summit heights are $(\rho\kappa c_p)'' = 1.0 \times 10^{-4}$ J²/cm⁴K²s, $\epsilon'' = 0.30$, and $G'' = 90$MPa. The symbols are the relaxation frequencies for α (○), β (◇), and *a* (□) process as obtained from the isotherms (see text).

however, remains nearly unaffected. It is mainly caused by changes of the phase angle φ.

The isochronous presentation has a disadvantage: Isochrones do not represent a thermodynamic state. The latter is defined by isotherms. The $\rho\kappa c_p''(\log f, T)$ contour map (Figure 4b) shows that the difference between isochrones and isotherms is important in the crossover region. Two clearly distinct processes, surprisingly separated by a saddle at ($\log(f/\mathrm{Hz}) = 0.33$, $T = 2$ °C), can be observed in the calorimetric contour map. The two processes are not simultaneously visible in the isochrones (Figure 3a).

The contour map of the dielectric loss compliance $\epsilon''(\log f, T)$ of PnHMA has no saddle (cross in Figure 4a). There is also no saddle in the contour map for the dynamic shear loss modulus $G''(\log f, T)$ (Figure 4c). The separation of α and β relaxation at low temperatures is only indicated by a significant broadening of the isothermal frequency range where the ϵ'' and G'' values are large. The ϵ'' and G'' isotherms in Figure 5 reflect the development of an independent α relaxation only by a systematic increase of the low frequency wing of the loss peaks with decreasing temperature.

The $\rho\kappa c_p''$ isotherms in Figure 6, called the "spectra" for short, show that the intensity of the high temperature process, called *a*, dies off above the saddle (Figure 6a), while a new relaxation process, the dynamic glass transition α, sets on below the saddle (Figure 6b). The intensity of the α relaxation increases with decreasing temperature. When the *isothermal* calorimetric relaxation frequencies are transferred into the contour plot (symbols in Figure 4b), we see that the high temperature relaxation *a* dies off at about $\log(f/\mathrm{Hz}) = 1.5$, about one frequency decade above the α onset.

The absence of a saddle in ϵ'' and G'' may provoke the question how significant this phenomenon is in $\rho\kappa c_p''$, i.e., how reproducible the small peak height of the 2 Hz isochrone is (Figure 3a). Three independent HCS

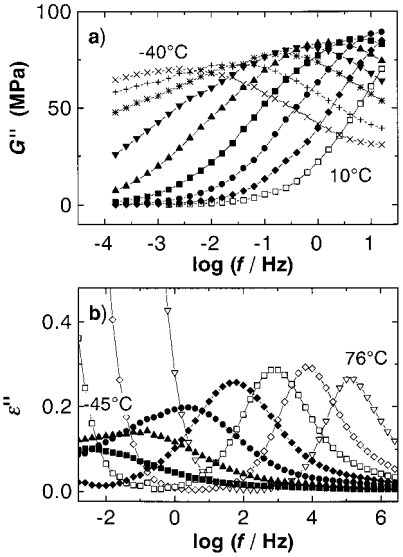

Figure 5. (a) Imaginary part of dynamic shear modulus G'' for PnHMA as a function of frequency at nine temperatures (×, −40 °C, +, −30 °C; *, −20 °C; ▼, −15 °C; ▲, −10 °C; ■, −5 °C; ●, 0 °C; ◆, 5 °C; □, 10 °C) and (b) the dielectric loss ϵ'' as a function of frequency at seven temperatures (■, −45 °C; ▲, −27 °C; ● −9 °C; ◆, 9 °C; □, 27 °C; ◇, 45 °C; ▽, 76 °C).

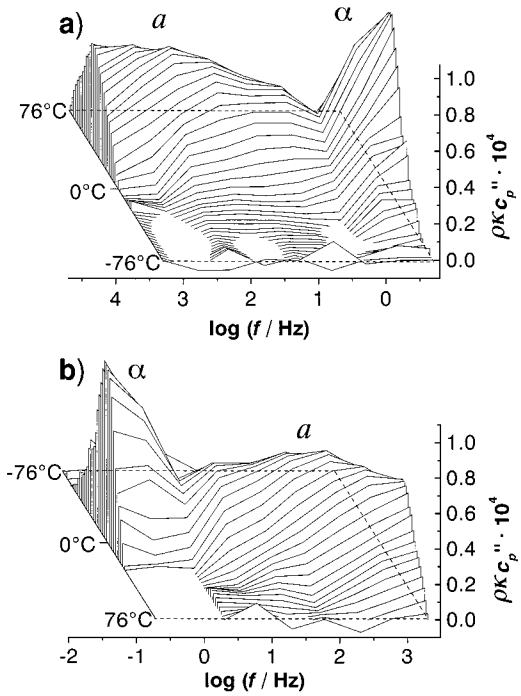

Figure 6. Isothermal sections of the imaginary-part surface $c_p''(\log f, T)$ for $T = -76$ °C (+3K) +76 °C in PnHMA. According to the fluctuation dissipation theorem (FDT), $c_p''(\omega)$ for any given temperature is proportional to the spectral density of entropy fluctuations, $\Delta S^2(\omega)$:$k_B c_p''(\omega) = \pi\omega\Delta S^2(\omega)$. The isothermal sections represent, therefore, the "entropy fluctuation spectra" at the dynamic glass transition: (a) seen from the low-temperature side showing the "death" of the *a* process; (b) seen from the high-temperature side showing the "onset" of the α process.

measurements with heaters of different geometry, all at a frequency of 2 Hz are compared in Figure 7. The empty substrates were separately measured, the base lines were independently determined (Figure 7a), and different temperature programs were used. Nevertheless, all curves coincide (Figure 7b). The peak height $\rho\kappa c_{p_{\max}}''$ is significantly lower, and the δT value is

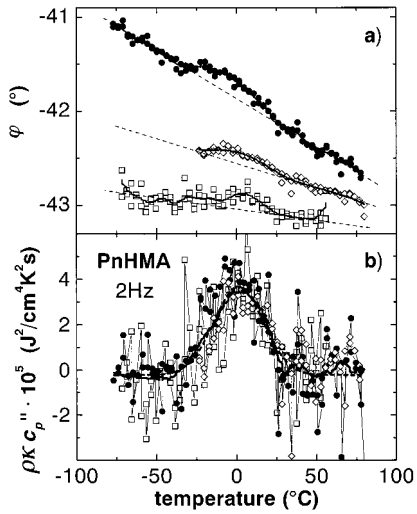

Figure 7. HCS data for PnHMA at a frequency of 2 Hz. The different symbols represent independent runs on the small (◇, ●) and the large nickel heater (□). (a) Raw phase angle φ vs temperature as calculated from the 3ω signal. The data were FFT filter smoothed (solid lines) and a linear base line was constructed (dashed lines). (b) The imaginary part $\rho\kappa c_p''$ vs. temperature as calculated from the three φ curves in part a. The solid line is a FFT filter smoothed curve. The dotted line is a fit to the data with a Gaussian function.

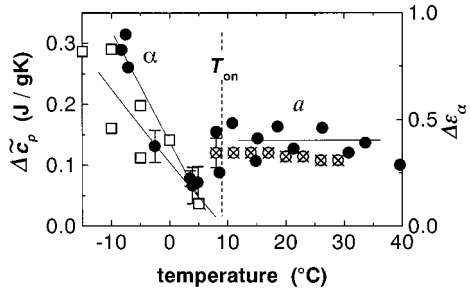

Figure 8. Calorimetric intensity (●, ⊗) and dielectric α intensity (□) as function of temperature for PnHMA. The calorimetric intensity was calculated from the imaginary part $\rho\kappa c_p''$ by the Kramers−Kronig relation: directly from $\rho\kappa c_p''$ isotherms (⊗) or from isochrones by a transformation of the Kramers−Kronig relation in the temperature domain (●, see text). A linear extrapolation of the α intensities gives α onsets at $T = 9 \pm 10$ °C and $T = 8 \pm 10$ °C for $\Delta\epsilon_\alpha$ and $\Delta\tilde{c}_p$, respectively.

smaller, than for the neighbor frequencies (see Table 2). A peculiarity of the equilibrium calorimetric trace in the Arrhenius diagram at about $T = 5$ °C was also confirmed by a modified Narayanaswamy model evaluation of the DSC curve.[30]

The calorimetric relaxation strength $\Delta\tilde{c}_p(T)$ as function of temperature was calculated from the isochrones of the imaginary part $\tilde{c}_p''(T)$ using the Kramers Kronig relation transformed into the temperature domain ($\Delta\tilde{c}_p(T) \approx (2/\pi)(\mathrm{d}(\ln f)/\mathrm{d}T)\int\tilde{c}_p''(T)\mathrm{d}T$). The $\Delta\tilde{c}_p$ values were adjusted by a fixed factor to absolute c_p values from the conventional DSC measurement as described above. At high temperatures ($T > T_{on}$) a nearly constant value of $\Delta\tilde{c}_p \approx 0.12$ J g^{-1} K^{-1} was observed for the *a* process, while below the α onset ($T < T_{on}$) a linear increase of the α relaxation strength $\Delta\tilde{c}_p$ with decreasing temperature is indicated (Figure 8). A linear[20] extrapolation to a calorimetric α onset temperature ($\Delta c_p(T_{on}) = 0$) gives $T_{on} = +8 \pm 10$ °C. Beside the evaluation of the isochrones, the calorimetric relaxation strength of the *a* process was also calculated from the $\tilde{c}_p''$ isotherms

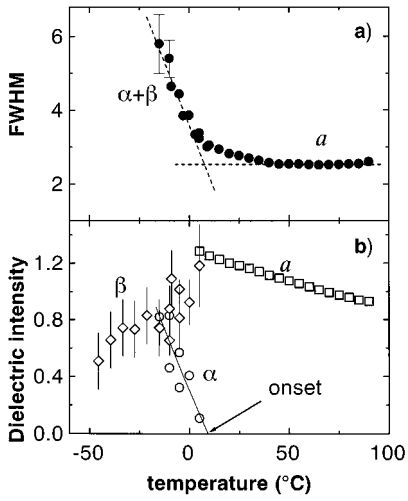

Figure 9. (a) Full width at half-maximum, fwhm, of the isothermal dielectric loss peaks as function of temperature for PnHMA. (b) Dielectric intensities $\Delta\epsilon$ of α (○), β (◇), and *a* (□) process as function of temperature obtained from fits to the isothermal data with one or the sum of two Havriliak−Negami functions (see text). The solid line indicates the linearity of the α intensity $\Delta\epsilon_\alpha(T)$.

using the Kramers Kronig relation (crossed open circles in Figure 8). Both procedures give consistent $\Delta\tilde{c}_p(T)$ values in the temperature range from 11 to 27 °C. Two additional Δc_p values are obtained from independent conventional DSC (nonequilibrium) measurements at a heating rate of +20 K/min: $\Delta c_p = 0.24$ and $\Delta c_p = 0.29$ J g^{-1} K^{-1} at $T_g = -18$ and -20 °C, respectively (not presented in Figure 8).

An extended analysis of the ϵ'' isotherms gives, in spite of the difference in the contour maps discussed above, a certain similarity of dielectric and calorimetric behavior. The increase of the dielectric full width at half maximum (fwhm) below the calorimetric onset temperature of 8 °C (Figure 9a) is an indication of the $\alpha\beta$ splitting in dielectric data.[21] Above $T \approx 20$ °C, the dielectric fwhm is nearly temperature independent and has a constant value of about 2.5 decades ($\beta_{KWW} \approx 0.45$). The $\rho\kappa c_p''$ peaks at comparable temperatures (*a* process) have a similar fwhm of about 2.5 decades. To get more information about the dielectric $\alpha\beta$ splitting, a sum of two Havriliak Negami (HN) functions,[34] $\epsilon^* - \epsilon_\infty = \Delta\epsilon(1 + (i\omega/\omega_0)^b)^{-g}$, was fitted to the ϵ'' isotherms by a nonlinear regression method based on the Levenberg−Marquardt algorithm.[35] The procedure used, the presumed additivity of dielectric α and β compliances, and the typical features in the splitting region are discussed in previous papers.[9,10] Applied to PnHMA we get the following result: Above $T = 9$ °C acceptable fits could be obtained by using one single HN function for *a* (+ conductivity term). No systematic deviations were observed. Below 0 °C systematic deviations of a single-function HN fit from experimental data were obtained. Such a behavior is characteristic[9,10] for the $\alpha\beta$ splitting region and indicates the presence of two underlying relaxation processes. The ϵ'' isotherms for $T < 0$ °C were therefore fitted by a superposition of two HN functions and a conductivity term. The intensities of all three dielectric relaxations (*a*, α, and β) depend on the temperature (Figure 9b). The intensity of the α relaxation increases linearly with decreasing temperature. The extrapolation $\Delta\epsilon_\alpha \rightarrow 0$ gives a dielectric onset temperature T_{on} of 9 ± 10 °C coincident with the calorimetric onset at 8 ± 10 °C (Figure 8).

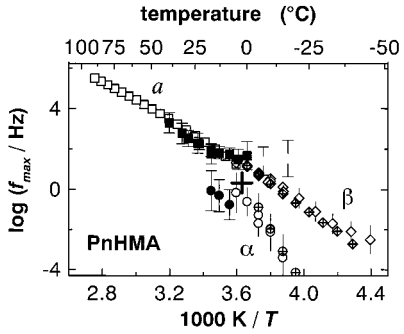

Figure 10. Arrhenius diagram for PnHMA. The frequency position of the peak maxima of *a* (squares), α (circles), and *β* (diamonds) processes from dielectric spectroscopy (open symbols) and dynamic shear modulus (cross at center). The isothermal HCS peak maxima (full symbols) for α and *a* are shown for comparison. The gray *a* points stem from very small intensities; *β* is absent in HCS data. The cross (+) indicates the saddle point in the calorimetric contour map (Figure 4b).

The dielectric loss peak maxima frequencies f_{max} of PnHMA for all three relaxation processes (*a*, α, and *β*) are transferred into an Arrhenius diagram, log f_{max} vs reciprocal temperature, $1/T$ (Figure 10), and the dielectric contour map (Figure 4a). The α intensity onset is about one frequency decade below a quasi-continuous *aβ* trace. The *a* and α traces are slightly curved, while the *β* trace is a straight line, as expected for a local process.

The shear loss maxima for the different processes as obtained from logarithmic Gauss fits to the G'' isotherms and the isothermal $\rho\kappa c_p''$ maxima from Figure 4b are added in Figure 10. The comparison of the isothermal peak frequencies from the three different responses shows good agreement for the α and *a* processes. With respect to the different shape of the $\epsilon''(\log f, T)$ and $\rho\kappa c_p''(\log f, T)$ surfaces the large degree of coincidence seems surprising. The difference between the contour maps of ϵ'' and $\rho\kappa c_p''$ is caused by the different activities of the local *β* relaxation: The large dielectric *β* activity hides the α onset. The latter is, however, clearly seen in the calorimetric contour map because *β* is calorimetrically inactive.

IV. Discussion

The main experimental finding is a separate α onset in the crossover region by both dielectric *and* heat capacity spectroscopy. While this onset can be obtained from dielectric data only by a fitting procedure, it can directly be seen as a saddlelike peculiarity in the calorimetric contour map. This saddle of the $\rho\kappa c_p''(\log f, T)$ surface can be described as follows: At high frequencies and temperatures, the *a* process is calorimetrically weakly active with a nearly constant intensity and shape. But its intensity dies off at a frequency of about $\log(f/\text{Hz}) = 1.5$, and a new process (α) sets on about one frequency decade below ($\log(f_{on}/\text{Hz}) \approx 0.3 \pm 0.5$). The intensity of the α process increases strongly below the onset. This view is supported by the agreement of the independently determined calorimetric and dielectric α onset points, by the temperature dependence of the α intensity from our dynamic shear data (not shown), and by an analysis of DSC measurements by a modified Narayanaswamy model.[30]

In order to discuss the crossover region in a more general context we will enlarge the experimental basis by results on some materials with similar chemical structure and relaxation behavior. In the homologous series of poly(*n*-alkylmethacrylate)s the frequency-temperature position of the *αβ* splitting region shifts systematically downwards with increasing length of the side chain, due to internal plasticization.[22] We assume that this shift does not destroy the universality of the underlying α, *β*, and *a* relaxation mechanisms in the crossover region of our substance class. A calorimetric α onset can also be extrapolated from HCS data on random copolymers P(nBMA-*stat*-S)[10] and PnBMA[32,36] having slightly higher crossover frequencies ($\log(f_{on}/\text{Hz}) \approx 3$). Below this onset, both the calorimetric and the dielectric intensity of the α process increase linearly as it is indicated for PnHMA in Figure 8. By plotting the calorimetric intensities of α and *a* processes vs reduced temperature ($T_{on} - T$) for several random copolymers and PnHMA in one diagram, we obtain a masterplot (Figure 11a) which visualizes the calorimetric behavior in the crossover region of our substance class. The onset temperatures T_{on} for the copolymers were extrapolated from dielectrics, $\Delta\epsilon_\alpha \rightarrow 0$ for $T \rightarrow T_{on}$. There are two ranges with clearly distinct behavior: (i) the temperature range of the *a* process ($T > T_{on}$) where Δc_p is small and nearly constant and (ii) the α region below the onset temperature ($T < T_{on}$) with a linear increase of $\Delta\tilde{c}_p$ as function of temperature, i.e., $\Delta\tilde{c}_p \sim (T_{on} - T)$. The difference, if any, between dielectric and calorimetric onset temperatures is smaller than $\Delta T_{on} = 15$ K (Figure 11). This seems slightly outside the experimental uncertainty which mainly results from the uncertainty of extrapolation.

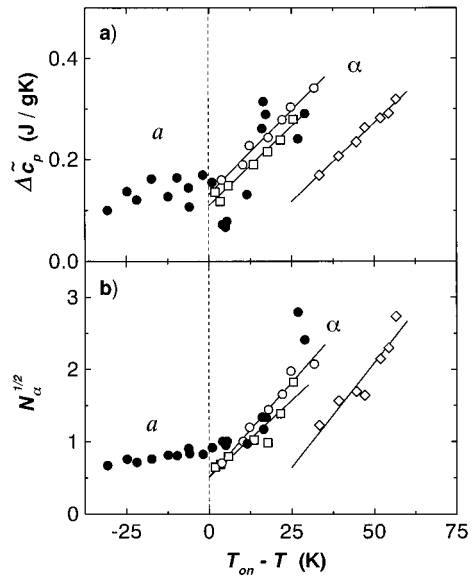

Figure 11. Calorimetric indication of the onset linearity. (a) The $\Delta\tilde{c}_p$ values for PnHMA from Figure 8 (●) are completed by two DSC points (see Table 2) and $\Delta\tilde{c}_p$ values of similar substances where the onset is slightly above the frequency window of HCS: random copolymers of nBMA with styrene for 2% mole S (□), 8% S (○), and 19% S (◇).[10] (b) The square root of cooperativity, $N_\alpha^{1/2}$, as evaluated by eq 1 from HCS data for the same substances. The onset temperatures are from dielectrics.

Now we introduce the cooperativity concept in the discussion. From the calorimetric contour map we see that the character of entropy fluctuation (i.e. of the cooperativity) changes abruptly in the crossover region. The size of cooperativity is quantified by using a fluctuation formula:[37,38]

$$N_\alpha = RT^2\,\Delta(1/c_V)/M_0(\delta T)^2 \approx RT^2\Delta c_p/M_0(\delta T)^2\,\bar{c}_p{}^2 \quad (1)$$

N_α is the volume of a cooperatively rearranging region, CRR, divided by the mean volume of a monomeric unit with molecular weight M_0 ($\approx$0.28 nm^3). For larger CRRs, N_α is the number of units within. Furthermore, Δc_p is the step height, δT the temperature fluctuation of one CRR determined as the Gaussian dispersion of the $c_p''(T)$ peak, $\bar{c}_p$ the mean value of c_p at half step height, and R the molar gas constant. The applicability of eq 1 to small N_α values down to $N_\alpha \approx 1$ is discussed in ref 20.

The calculated N_a values for PnHMA are listed in Table 2, together with the experimental Δc_p and δT values. The square root of N_α as function of temperature is plotted for PnHMA and the copolymers in Figure 11b. All N_α values near the α onset temperature are about $N_\alpha = 1$. This is very small when compared with typical $N_\alpha \approx 50$ values far below the onset for glasses having crossover frequencies above MHz (Table 1). Different behavior above and below the α onset temperature is observed for the $N_\alpha{}^{1/2}(T)$ function: Above the onset the N_α values weakly depend on temperature and are smaller than one. Below the onset, $T < T_{on}$, $N_\alpha{}^{1/2}$ increases linearly.

Small $N_\alpha \approx 1$ values are inconsistent with the interpretation of cooperativity as a motion of a larger number of particles which are, in a way, coupled in space and time, at least if we think about the monomeric unit as a "particle". The temperature dependence of our $N_\alpha(T)$ and $\Delta c_p(T)$ functions suggests the following interpretation: Above the onset ($T > T_{on}$) parts of few monomeric units (also from different chains) act together to make the *a* process with a small residual entropic activity. We suggest the term "coordinative" here in the sense that coordination means a harmonious functioning of parts for most effective result. This includes, of course, orientational dependence of intermolecular potentials and perhaps participation of intramolecular degrees of freedom. Below the onset ($T < T_{on}$) the α cooperativity increases, and more and more intermolecular possibilities come into the play ($N_a > 1$). This means that a qualitative change from coordinative motions above T_{on} (high temperature *a* process) to intermolecular cooperativity below T_{on} (low temperature α process) is observed in the crossover region. The qualitative difference between *a* and α[39] is indicated by the saddle in the calorimetric contour map (Figure 4b) and the separate α onset in the Arrhenius diagram (Figure 10). A highly cooperative α relaxation in the classical sense is restricted to temperatures far below T_{on}. It is such an α relaxation that usually freezes-in near the glass temperature T_g. The main difference may be a thermokinetic structure[38,40] in case of α which is probably absent for an *a* process. A physical picture describing the similarities and differences of α and *a* is discussed in ref 30.

Finally, we will assembly some arguments why we believe that an onset of α relaxation and intermolecular cooperativity is a general phenomenon in the crossover region of glasses: (i) A *dielectric* α onset has been observed in several (poly(*n*-alkyl methacrylate)s[9,41] and their random copolymers with styrene,[10] epoxy resins,[11,12] polybutadiene,[13] and toluene.[14] (ii) A *calorimetric* onset was observed for glasses having the crossover in the HCS frequency window (PnHMA and PnBMA[36] and its random copolymers with styrene[10]). A general calorimetric α onset is indicated by the finding that the calorimetric α relaxation strength $\Delta c_p(T)$ decreases with increasing temperature for many glasses.[21,25,27,33] The opposite case has never been observed. In the extrapolation $\Delta c_p(T) \rightarrow 0$ modulated calorimetry yields a calorimetric α onset point (log f_{on}, T_{on}).[42] (iii) Although there are several substances,[43] where the dielectric relaxation strength $\Delta\epsilon_\alpha$ does not tend to zero in the crossover region, first HCS measurements on such a substance indicate a cooperativity onset also in such glasses. The experiments were done on the good glass former benzoisobutyl ether, BIBE,[44] having the crossover in the 10 kHz range.

V. Conclusions

The crossover from the high temperature *a* process to the classical low temperature α process in PnHMA was investigated by heat capacity spectroscopy. The high temperature *a* process is connected with coordinative molecular motions on a length scale <1 nm, while the α relaxation is characterized by an increasing intermolecular cooperativity arriving at length scales >1 nm far below the onset. These length scales depend upon the condition that eq 1 is reasonable for the α and *a* process. We observed that the *a* and α processes are not continuously connected, but are separated by a saddle of less calorimetric activity. We found a death of the *a* process which is clearly separated from an onset of the α process. The frequency gap is of order one frequency decade. This gap is supported by an additive analysis of dielectric compliance. There is increasing evidence that a calorimetric α onset can be observed not only in some exotic materials but also in the conventional glass formers with crossover frequencies above MHz. We think that not only the extrapolation of mode coupling theory[45] to low frequencies but also the extrapolation of cooperativity concepts to high frequencies will lead to an inadequate description of the relevant relaxation mechanisms. Instead, the main transition in glasses seems to consist of two calorimetrically distinct parts, just the high temperature *a* process and the low temperature α process, which need different concepts for molecular understanding.

Acknowledgment. The authors thank the Deutsche Forschungsgemeinschaft DFG, the Fonds Chemische Industrie FCI, and the Land Sachsen-Anhalt for financial support.

References and Notes

(1) 1st International Discussion Meeting on Relaxations in Complex Systems, Crete, Greece, 1991. *J. Non-Cryst. Solids* **1991**, *131−133*.
(2) 2nd International Discussion Meeting on Relaxations in Complex Systems, Alicante, Spain, 1994. *J. Non-Cryst. Solids* **1994**, *172−174*.
(3) 3rd International Discussion Meeting on Relaxations in Complex Systems, Vigo, Spain, 1997. *J. Non-Cryst. Solids* **1998**, *235−237*.
(4) Adam, G.; Gibbs, J. H. *J. Chem. Phys.* **1965**, *43*, 139.
(5) Johari, G. P.; Goldstein, M. *J. Chem. Phys.* **1970**, *53*, 2372; **1971**, *55*, 4245; *J. Phys. Chem.* **1970**, *74*, 2034. Johari, G. P. *Ann. N.Y. Acad. Sci.* **1976**, *279* , 117.
(6) Barlow, A. J.; Lamb, J.; Matheson, A. J. *Proc. R. Soc. London, Ser. A* **1966**, *292*, 322. Cukierman, M.; Lane, J. W.; Uhlmann, D. R. *J. Chem. Phys.*, **1973**, *59*, 3639. Laughlin, W. T.; Uhlmann, D. R. *J. Phys. Chem.* **1972**, *76*, 2317.
(7) Stickel, F.; Fischer, E. W.; Richert, R. *J. Chem. Phys.* **1995**, *102*, 6251; **1996**, *104*, 2043. Hansen, C.; Stickel, F.; Berger, T.; Richert, R.; Fischer, E. W. *J. Chem. Phys.* **1997**, *107*, 1086.

(8) Fujara, F.; Geil, B.; Sillescu, H.; Fleischer, G. *Z. Phys. B* **1992**, *88*, 195.
(9) Garwe, F.; Schönhals, A.; Lockwenz, H.; Beiner, M.; Schröter, K.; Donth, E. *Macromolecules* **1996**, *29*, 247.
(10) Kahle, S.; Korus, J.; Hempel, E.; Unger, R.; Höring, S.; Schröter, K.; Donth, E. *Macromolecules* **1997**, *30*, 7214.
(11) Casalini, R.; Fioretto, D.; Livi, A.; Lucchesi, M.; Rolla, P. A. *Phys. Rev. B* **1997**, *56*, 3016.
(12) Corezzi, S.; Capaccioli, S.; Gallone, G.; Livi, A.; Rolla, P. A. *J. Phys.: Condens. Matter* **1997**, *9*, 6199.
(13) Arbe, A.; Richter, D.; Colmenero, J.; Farago, B. *Phys. Rev. E* **1996**, *54*, 3853.
(14) Kudlik, A.; Tschirwitz, C.; Benkhof, S.; Blochowicz, T.; Rössler, E. *Europhys. Lett.* **1997**, *40*, 649.
(15) Sokolov, A. P. *Endeavour* **1997**, *21*, 109.
(16) Kishimoto, K.; Suga, H.; Seki, S. *Bull. Chem. Soc. Jpn.* **1973**, *46*, 3020.
(17) Fan, J.; Cooper, E. I.; Angell, C. A. *J. Phys. Chem.* **1994**, *98*, 9345.
(18) It is still controversially debated if the dielectric compliances of α and β process are additive[9,11,14] or if the multiplicative Williams ansatz in the time domain[13,23] must be used. The second forces a continuous merging of α and β relaxation in the crossover region. (see also: Donth, E.; Schröter, K.; Kahle, S. Comment on Merging of the α and β relaxations in polybutadiene: A neutron spin echo and dielectric study. Submitted for publication in *Phys. Rev. E*).
(19) Hempel, E.; Beiner, M.; Renner, T.; Donth, E. *Acta Polym.* **1996**, *47*, 525.
(20) Donth, E.; Kahle, S.; Korus, J.; Beiner, M. *J. Phys. I Fr.* **1997**, *7*, 581.
(21) Beiner, M.; Korus, J.; Donth, E. *Macromolecules* **1997**, *30*, 8420.
(22) Heijboer, J. In *Physics of Non-Crystalline Solids*; Prins, J. A., Ed.; North-Holland: Amsterdam, 1965; p 231.
(23) Williams, G.; Watts, D. C. *Trans. Faraday Soc. II* **1971**, *67*, 2793.
(24) Beiner, M.; Garwe, F.; Schröter, K., Donth, E. *Colloid Polym. Sci.* **1994**, *272*, 1439.
(25) Birge, N. O.; Nagel, S. R. *Phys. Rev. Lett.* **1985**, *54*, 2674; *Rev. Sci. Instrum.* **1987**, *58*, 1464.
(26) Birge, N. O.; Jeong, Y. H.; Nagel, S. R. *Ann. N.Y. Acad. Sci.* **1986**, *484*, 101.
(27) Korus, J.; Beiner, M.; Busse, K.; Kahle, S.; Unger, R.; Donth, E. *Thermochim. Acta* **1997**, *304/305*, 99.
(28) Giebel, L.; Meier, G.; Fytas, G.; Fischer, E. W. *J. Polym. Sci., Part B: Polym. Phys.* **1992**, *30*, 1291.
(29) Meier, G.; Kremer, F.; Fytas, G.; Rizos, A. *J. Polym. Sci., Part B: Polym. Phys.* **1996**, *34*, 1391.
(30) Kahle, S.; Hempel, E.; Beiner, M.; Unger, R.; Schröter, K.; Donth, E. *J. Mol. Struct.*, in press.
(31) Heijboer, J. *Stat. Dyn. Prop. Polym. Solid State* **1982**, *94*, 197.
(32) Korus, J. Thesis, Universität Halle, 1997.
(33) Birge, N. O.; Menon, N. *Thermochim. Acta* **1997** , *304/305*, 51. Birge, N. O. *Phys. Rev. B* **1986**, *34*, 1631.
(34) Havriliak, S.; Negami, S. *J. Polym. Sci. C* **1966**, *14*, 99.
(35) Press, W. H.; Flannery, B. P.; Teukolsky, S. A.; Vetterling, W. T. *Numerical Recipes in Pascal (Fortran, C). The Art of Scientific computing;* Cambridge Univ. Press: Cambridge, England, and New York, 1992.
(36) Gutewort, K. Universität Halle. Unpublished results.
(37) Donth, E. *J. Non-Cryst. Solids* **1982**, *53* , 325.
(38) Donth, E. *Relaxation and Thermodynamics in Polymers. Glass Transition;* Akademie-Verlag: Berlin, 1992.
(39) Williams, G. *Trans. Faraday Soc.* **1966**, *62* , 2091.
(40) Donth, E. *J. Polym. Sci., Part B: Polym. Phys.* **1996**, *34*, 2881.
(41) Garwe, F.; Schönhals, A.; Beiner, M.; Schröter, K.; Donth, E. *J. Phys.: Condens. Matter* **1994**, *6*, 6941.
(42) Korus, J.; Hempel, E.; Beiner, M.; Kahle, S.; Donth, E. *Acta Polym.* **1997**, *48*, 369.
(43) Schönhals, A; Kremer, F. *J. Non-Cryst. Solids* **1994**, *172−174*, 336.
(44) Kahle, S.; et al., to be submitted for publication.
(45) Götze, W.; Sjögren, L. *Rep. Prog. Phys.* **1992** , *55*, 241.
(46) Beiner, M.; Korus, J.; Lockwenz, H.; Schröter, K.; Donth, E. *Macromolecules* **1996**, *29*, 5183.

MA980754M